New Methods to Transport Fluids in Micro-Sized Devices

Shaun Berry and Jakub Kedzierski

Applications of microfluidics require a self-contained, active pumping system in which the package size is comparable to the volume of fluid being transported. Over the past decade, several systems have been developed to address this issue, but either these systems have high power requirements or the microfabrication is too complex to be cost efficient. A recent effort at Lincoln Laboratory using an emerging technology called electrowetting has led to the development of several novel micropump concepts for pumping liquids continuously, as well as for pumping discrete volumes.

Microfluidics encompasses the science and technology of systems that process or manipulate extremely small volumes of fluids, generally ranging from nanoliters to attoliters (10^{-9} to 10^{-18} liters). Applications span from physical-science-based applications such as inkjet printers and microfuel cells to biotechnology applications such as DNA analysis and drug discovery. The appeal of microfluidics, particularly in biotechnology, is the ability to separate and detect cells, molecules, and other entities and to perform analyses more quickly and with increased sensitivity, automation, and parallelization. Moreover, the reduction in reagent and sample volumes means less cost per analysis [1]. Such miniaturization also opens up the possibility of developing portable devices for medical diagnostic tools or environmental monitors.

However, the miniaturization of fluid systems poses significant challenges. For example, the fundamental task of integrating fluid into a micro-sized device can be difficult because fluid-handling tools required to go from the macro-world to the micro-world are not yet well established. In addition, the ability to precisely control and transport fluid in micro-sized structures presents its own unique set of challenges.

At the root of these challenges is fundamental fluid physics. For devices in which feature dimensions are on the scale of micrometers and fluid volumes on the order of nanoliters, surface tension, viscosity, and electrical charges become dominant forces over inertial forces. As a consequence, performing the basic fluidic operations that are essential to the functionality of the system—such as fluid transport, mixing, and filtering—requires

unorthodox and innovative approaches.

In a large number of microfluidic systems, fluids are transported by pressure gradients generated from pumps external to the device. In these types of systems, the overall size is dominated by the size of the external pumping components, which are typically large relative to the microfluidic device itself. This approach may be suitable for a broad range of applications; a key factor for a truly miniaturized system, however, is to have a self-contained pumping and fluid transport system [2]. Systems that generate pressure on chip have been based on a wide range of effects, including electro-osmosis [3, 4], electrophoresis [5], electromagnetism [6], acoustics [7], and thermocapillary effects [8]. In addition, self-contained micropumps have been developed that consist of moving solid boundaries in microelectromechanical systems, or MEMS [2, 9, 10].

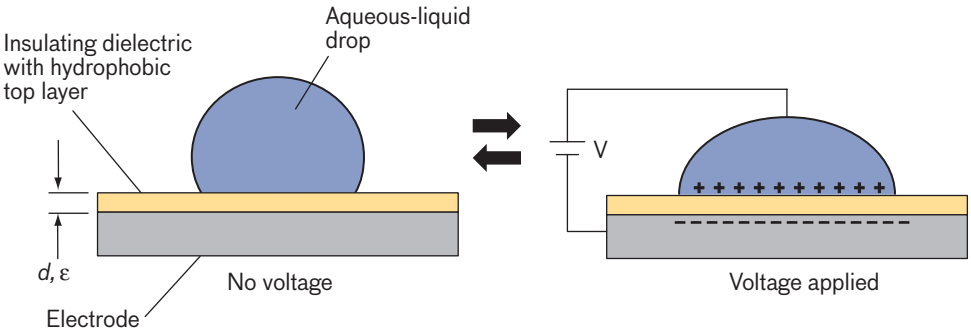

FIGURE 1. Electrowetting works by using an electric voltage to deform a liquid drop. At left is the basic electrowetting setup, with a sessile drop on a dielectric-coated electrode. At right, the drop flattens and wets the surface when an electrical potential is applied. The quantities *d* and ε represent the dielectric thickness and dielectric constant. When the potential is removed, the drop returns to its original configuration.

One technique that can be used to manipulate fluids on the microscale is electrowetting. Electrowetting refers to the phenomenon in which the wetting property, i.e., surface tension, of a conductive liquid on a dielectric-coated electrode is altered because of an applied electrical potential [11–13]. The most common configuration associated with electrowetting, as depicted in Figure 1, consists of a drop of an aqueous liquid, typically on the order of 1 to 2 millimeters in diameter, positioned on a solid electrode surface insulated with a thin dielectric material that in most applications ranges in thickness from a few nanometers to a few hundred micrometers. The dielectric material, if not hydrophobic, is coated with a thin hydrophobic polymer layer. The inclusion of the hydrophobic layer improves electrowetting behavior. The application of an electrical potential between the solid electrode and the liquid drop results in the drop flattening and wetting over the surface, as shown in Figure 1. What is appealing about this phenomenon is that it is reversible: after the potential is removed, the drop returns to its original configuration. In essence, electrowetting can be thought of as a technique to actively control the deformation of a liquid surface.

Electrowetting applications such as variable focus lenses [14–16] and liquid displays [17–20] are developed to take advantage of this control in surface deformation. However, these applications produce no net-positive movement or flow of fluid. Liquid transport using electrowetting techniques has, up until now, been limited to the transport of discrete volumes, i.e., droplets on the order of nanoliters. This approach to liquid manipulation, called digital microfluidics, has several advantages: there are no moving parts, multiple drops can be independently controlled, it is electronically reconfigurable, and it makes efficient use of the sample and reagent volumes [21–25].

Systems of this kind typically sandwich drops between two parallel plates separated by a small gap (nanometers to micrometers). Arrays of electrodes, insulated with a thin dielectric, are patterned over the surface of one of the plates. Individual liquid drops are transported by the proper sequencing of a voltage potential on the array of patterned electrodes. Critical fluidic functions such as transporting, merging, splitting, and mixing of drops have been demonstrated by this method [23]. Current research in biological applications using digital electrowetting includes polymerase chain reaction (PCR) for DNA analysis [26], assays [27], and protein analysis [28].

While this type of design is easy to fabricate, it limits the types of fluidic functions that can be implemented. For example, these systems are not pumping fluid in a classical sense, in which a pressure gradient is used to generate flow. Since these are open systems, the structures

Fabricating a Micropump

The microfluidic structure developed to take advantage of the electrowetting effect consists of two microfabricated wafers, bonded together with enclosed microchannels and electrowetting-controlled fluidic devices in between (see diagram, below). The 6-inch-diameter silicon wafer on the bottom has the electrodes and electrical contacts fabricated on it, with fluidic input/output ports drilled through. The 4-inch-diameter top wafer is made of Pyrex, which allows for optical observation of the liquids in the microchannels.

Bottom Wafer

First, a 2-μm-thick layer of SiO_2 is deposited by plasma-enhanced chemical vapor deposition (PECVD). Next, the electrode layer is formed by depositing and patterning a 300-nm-thick layer of aluminum. A layer of SiO_2 is then deposited and polished by chemical mechanical planarization (CMP) to a thickness of 2 μm. After CMP, the electrical-contact-pad openings are patterned and wet-etched in hydrofluoric acid.

The microchannel layer is then formed by a 11-μm-thick patterned SU-8 photoresist. Next, a hydrophobic, amorphous fluoropolymer layer (aFP) film is spun on the wafer so that the aFP covers the top of the SU-8, including the channel side and bottom walls. The aFP used is 3% Cytop (CTL-809M from Asahi Glass) suspended in a perfluorinated solvent. After spinning, the wafer is baked at 90ºC for 30 s to evaporate the remaining solvent, resulting in a 200-nm-thick film. This layer is further hardened by vacuum baking at 150ºC for 1 min.

In the final process step, an ultrasonic drill creates 2-mm-diameter fluidic ports through the wafer. A thick photoresist layer protects the Cytop layer from damage during the drilling and is removed with acetone after drilling.

Top Wafer

First, the microchannel layer is formed by a 11-μm-thick patterned SU-8 photoresist. Next, a transparent 100 nm layer of indium-tin-oxide (ITO) is sputtered onto the wafer; finally, 2% Cytop is spun on the wafer and baked. The Cytop application process is the same as that used for the bottom wafer, except in this case the film is only 80 nm thick.

Bonding

The final microfluidic structure is formed by thermally bonding the Cytop surfaces of the two wafers. The bond is formed by applying pressure to the top of the Pyrex wafer at 150ºC. After bonding, liquid connections are made with NanoPort assemblies (Upchurch Scientific), which are epoxied to the bottom of the silicon wafer. The NanoPorts are a threaded component that allows for standard-size tubing to be conveniently connected. In this design, we attach 1-mm-diameter Teflon tubing.

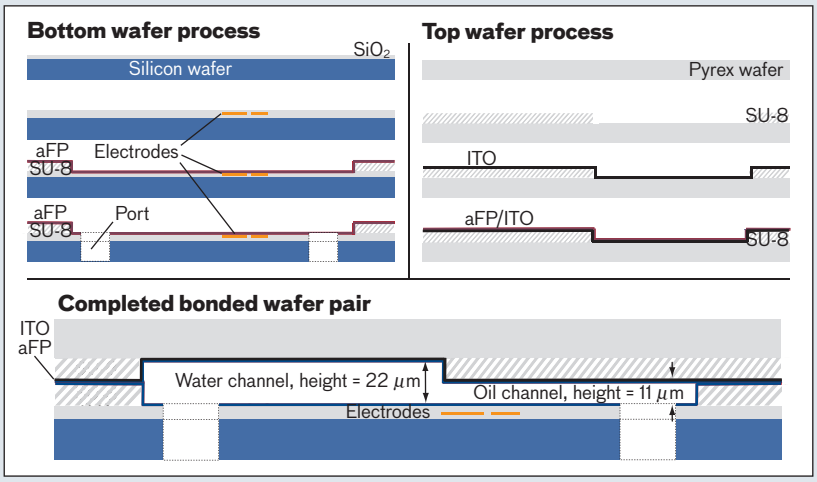

FIGURE A. The electrowetting microchannels are sandwiched between a silicon bottom wafer and a Pyrex top wafer.

have no flow channels; thus no positive pressure can be achieved. The motivation for our work is to take advantage of electrowetting's key attributes (low power, lack of moving solid parts, and small size) and apply them for transporting liquids in closed-microchannel structures. Deforming a liquid interface in a closed microchannel creates the pressure gradients required to drive fluid motion. The ability to do pressure work in a closed microchannel will enable the development of integrated micropumps, as well as other devices that form valves, pistons, and drop generators—all the essential elements required in microfluidic systems.

Design

The idea behind the devices fabricated was to use the mechanical work resulting from the displacement of the liquid interface to do pressure work. All the fluidic devices were designed to operate by using two immiscible liquids: water as the conductive liquid and low-viscosity oil (in particular, dodecane oil) as an insulating liquid. We have already studied the electrowetting properties of this two-liquid system [29–31]. The use of an oil phase prevents evaporation and limits hysteresis effects that often arise in water-gas microchannel systems [32].

The microfluidic structure consisted of two microfabricated wafers bonded together with enclosed microchannels and electrowetting-controlled fluidic devices in between. The overall structure we developed during this research is shown in Figure 2. Details of the fabrication process are described in the sidebar "Fabricating a Micropump" (page 72).

Individual fluidic devices were grouped into six fluid independent substructures, or zones. Each zone had two liquid access ports, a single aqueous-water fill port, and a single oil fill port. In each zone, the individual fluidic devices are tied to liquid feed channels—one for the water phase and one for the oil phase. Each device in a zone was designed to be independently operated.

Principle of Operation

The structure is initially filled with dodecane oil. This process happens immediately once the oil enters one of the ports, because the oil-fluoropolymer surface energy is much smaller than the air-fluoropolymer surface energy. Once the structure is filled with oil, the water is introduced at the water port with a pressure P_b. The

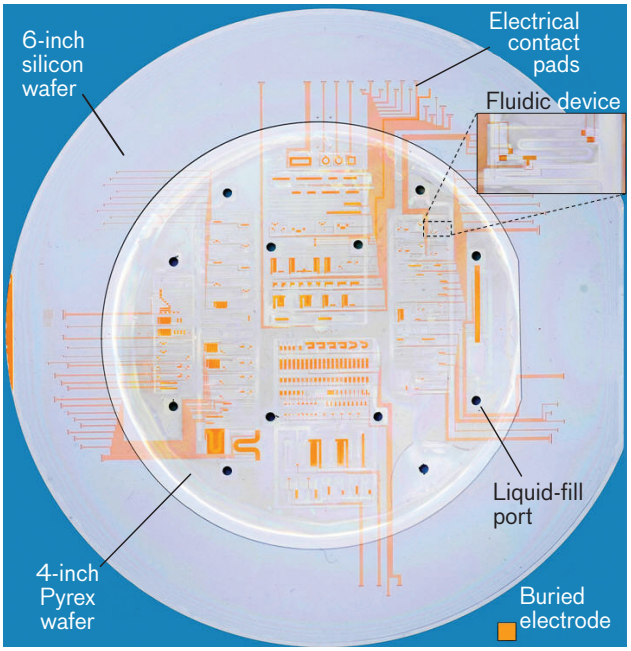

FIGURE 2. The microfluidic structure developed at Lincoln Laboratory, shown here in top view, consists of two microfabricated wafers bonded together: a 6-inch-diameter silicon wafer (bottom) and a 4-inch-diameter Pyrex wafer (top). All microchannels and fluidic devices are located between the wafers.

water pressure is controlled with a manometer with a pressure range of 0 to 15 kPa. Since all the surfaces of the fluidic channels are coated with Cytop, a hydrophobic material, a positive pressure is required to fill the channel with water. The pressure required to force water into a hydrophobic microchannel is a function of the surface energy of the liquid interface and the geometry of the channel. In this design, the channels are much wider ($w \geq 100\ \mu$m) than they are high ($h = 11\ \mu$m for oil, 22 μm for water), with the result that the channel height is the dominant geometric parameter for determining the pressure required. On the basis of the Young-Laplace equation [33], the minimum pressure for the water phase to fill the water channels is $P_{min} = 4.5$ kPa. Since the oil channels are half the height of the water channels, roughly twice that water pressure—i.e., $P_{max} = 9$ kPa—is required for water to flow into them. Note that the pressures associated with this system are less than one tenth of an atmosphere. As long as P_b is kept between P_{min} and P_{max}, water will fill the water channels but not displace into the oil channels. During the actual filling of our structure, we maintained P_b at 5.5 kPa. This process

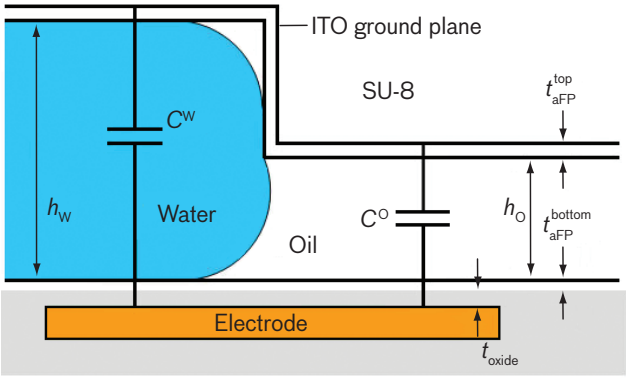

FIGURE 3. In a filled single-electrode device, the water-filled channels have a height h_w and the oil-filled channels have a height h_o. The water/oil interface is at the boundary of the two heights when $P_{min} < P_b < P_{max}$. C^w and C^o indicate the capacitances across the electrode and ground plane for each channel.

worked well to give a slow and controllable water fill. At this pressure, the water displaces oil from the water channels but not from the oil channels. Figure 3 shows a representative channel cross section of a filled single-electrode device prior to voltage actuation.

Single-Electrode Actuation. With P_b maintained between P_{min} and P_{max}, the water/oil interface stays located at the step in channel height, as shown in Figure 3. To actively control the position of the interface, electrowetting is used to advance the water phase into the lower-height oil channel. Key to predicting the electrowetting behavior in a microchannel is the capacitance. The capacitances per unit area from the top of the indium-tin-oxide (ITO) ground to the bottom electrode are C^w in the water channel and C^o in the oil channel. Because water is treated as a conductor, C^w does not depend on the channel height; oil, however, is not a conductor and so C^o does depend on channel height. The expressions for C^w and C^o can be found in Reference 34.

When the voltage is applied to the bottom electrode, electrowetting pressure is included through Lippmann's equation [11] in the Young-Laplace equation, where the pressure difference across the water/oil interface becomes

$$\Delta P = \frac{2\gamma_w^*}{h_o} - \frac{C^* V^2}{2h_o},$$

where γ_w^* is the difference in the water-fluoropolymer and oil-fluoropolymer surface energies and is approximately 50 mJ/m^2; h_o is the height of the oil channel, $C^* = C^w - C^o$; and V is the potential applied to the bottom electrode relative to the ITO ground. The first term on the right-hand side is the pressure across an interface, based on the channel geometry, and is the Young-Laplace equation. The second term on the right-hand side is the change in pressure due to electrowetting.

If $\Delta P = P_b$, there is no interface movement or liquid motion, since the pressure across the water/oil interface is balanced against the applied pressure. Thus no useful work is done. If $\Delta P \neq P_b$, then a working pressure is defined as $P_s = P_b - \Delta P$, where P_s is the pressure that causes the interface and liquids to move. If $P_s = 0$, meaning $\Delta P = P_b$, then there is no interface movement, because the pressure difference across the interface does no work. When V becomes sufficiently large to generate

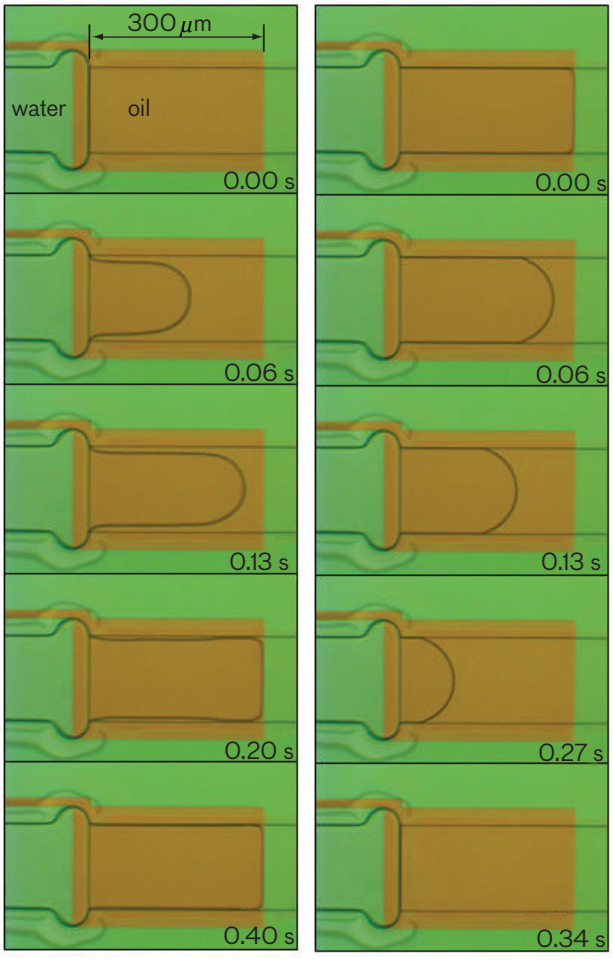

FIGURE 4. Top-down photographs show single-electrode actuation (left) and relaxation (right). The actuation voltage is 65 V dc and the pressure P_b is 8.0 kPa.

a positive P_s, it causes water to move into the oil channel. This voltage-induced actuation is shown in Figure 4 (left). As the figure shows, the interface advances only as far as the length of the electrode. With the water phase extended over the electrode, removal of the voltage causes ΔP to increase, which makes P_s negative and thus forces the water/oil interface back to its original position at the boundary between the water channel and the oil channel. This relaxation is shown in Figure 4 (right). Generally, the working pressure during actuation differs in magnitude from the working pressure during recession; as a result, the two processes occur at different speeds.

Directly measuring the actuation time and relaxation time with a charge coupled device (CCD) camera and considering the microchannel dimensions allow us to determine the flow rate for the two processes. Figure 5 shows a plot of flow rates, Q, for a single-electrode device for different actuation voltages and P_b values. During actuation, Q increases with higher P_b and V. During the return flow, however, Q decreases for higher P_b, which is independent of the voltage applied during actuation. The point where $Q = 0$ occurs when $P_s = 0$ and $P_b = \Delta P$. The intersection of the advancing flow-rate curves for a constant voltage with the return flow curve indicates the condition for which the two processes occur at the same speed.

By itself, the process of the interface advancing over the electrode and then receding is reversible, and therefore does no work. However, if we properly arrange the electrodes to control the flow, positive work can be done. It is through this concept of controlling the advancing interface and receding interface that pistons and valves have been developed and integrated into interesting devices such as pumps and drop generators.

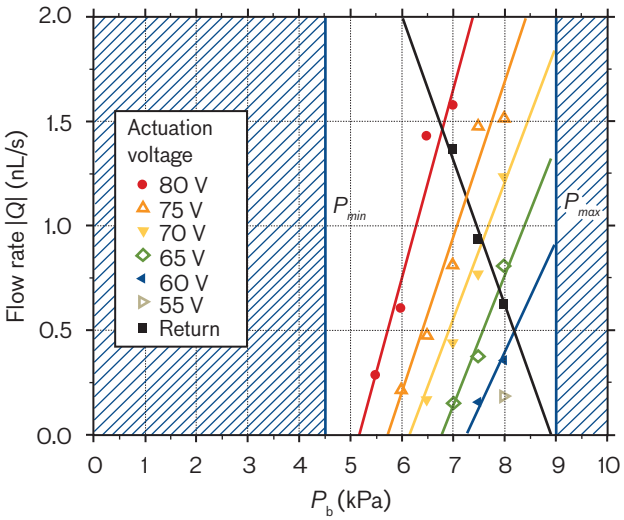

FIGURE 5. Turning up the DC actuation voltage increases the flow rate at a given pressure (P_b). Channel dimensions are w = 150 μm, h = 11 μm. The actuation shown in Figure 4 corresponds to the 65 V dc point at 8.0 kPa.

Micropumps

Micropumps are divided into two major categories: mechanical pumps and nonmechanical pumps. Mechanical pumps exert force on a working fluid by moving one or more boundaries. Nonmechanical pumps add momentum to the fluid by converting another energy form into kinetic energy. The electro-osmosis pump is an example of a nonmechanical pump [4]. The pumping concepts developed in this work are mechanical pumps, designed to operate in a periodic manner. Unique to our designs is that the moving boundaries are the liquid interfaces that are controlled through electrowetting. In one design, the micropump transports discrete volumes of water (individual drops) in a channel. Two other designs are for devices that would pump liquid continuously. These two designs differ in their working fluid—one uses a nonconductive liquid; the other uses water.

Design 1: Pumping Discrete Volumes. An integrated pumping system was developed to explore the concept of doing pressure work on individual drops in a closed microchannel by controlling the movement of water/oil interfaces with a mechanism analogous to a reciprocating piston pump. The transport system consisted of a drop generator and two pumps at the ends of a long microchannel. A drop generator can be used to create or destroy water drops in an oil channel. Figure 6 shows a sequence of images of a 0.5 nL water drop being created. In this design, two electrodes are used to form the drop generator. The drop generator creates drops and positions them in the microchannel. Once a drop is positioned in the oil channel, a pump at either end of the channel can move it. The pumps each consist of a valve and piston and can operate independently or in tandem.

Figure 7 shows eight drops that have been created and moved down an arbitrary long channel. The drops were transported with the right-side pump operating in "pull" mode. In this mode, the piston electrode is first activated, allowing the water to wet over the electrode.

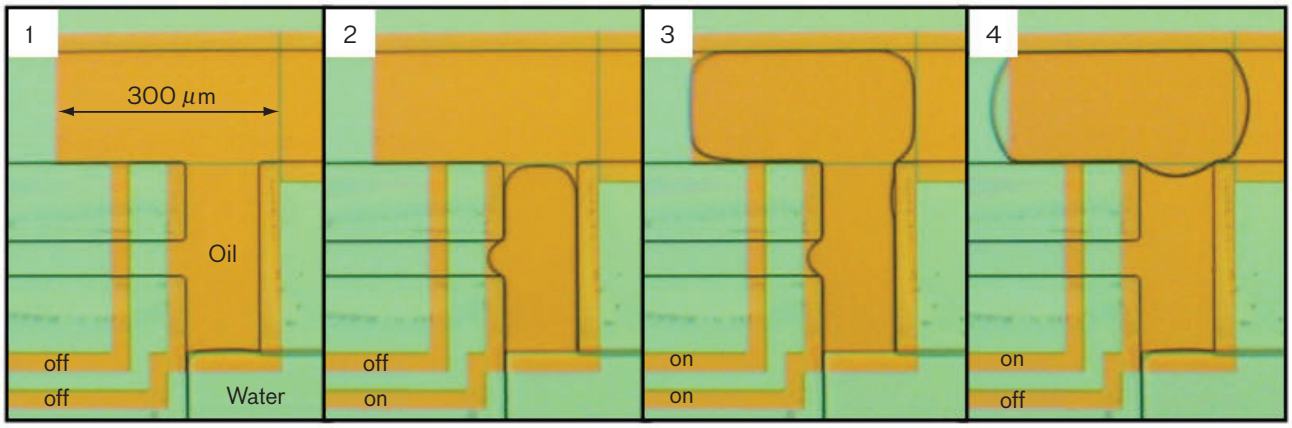

FIGURE 6. This series of top-down photographs shows a drop generator device creating a water drop. A reverse process (going from 4 to 1) can be used to destroy a drop. (V = 80 V dc; P_b = 7.5 kPa. Electrode-to-electrode spacing is 2 μm.)

With a potential still applied to the piston, the valve electrode is activated. A valve electrode functions by blocking the oil feed channel with water when a potential is applied (valve closed). When no voltage is applied, the valve is open. With the valve closed, the potential on the piston is removed. As a result, the interface over the piston is forced to retreat, pulling the drops down the channel. Unlike other digital microfluidic systems, this device requires only a few electrodes and is therefore less electrically complex. In addition, the drops move in a closed microchannel, an attribute that opens up a broader range of practical applications.

This pump can also operate in "push" mode, in which the valve is first closed (voltage applied to the electrode) and then the piston is actuated. This actuation pushes a drop or multiple drops down the channel.

Design 2: Oil Pump. The primary technique for using electrowetting to transport liquid is to control the movement of individual drops. As we have shown, this control can be accomplished by patterning an array of electrodes or through the pumping scheme described above. It is highly desirable, however, not just to move drops but to pump fluid continuously in a compact, self-contained system [2]. We have designed a device to demonstrate this

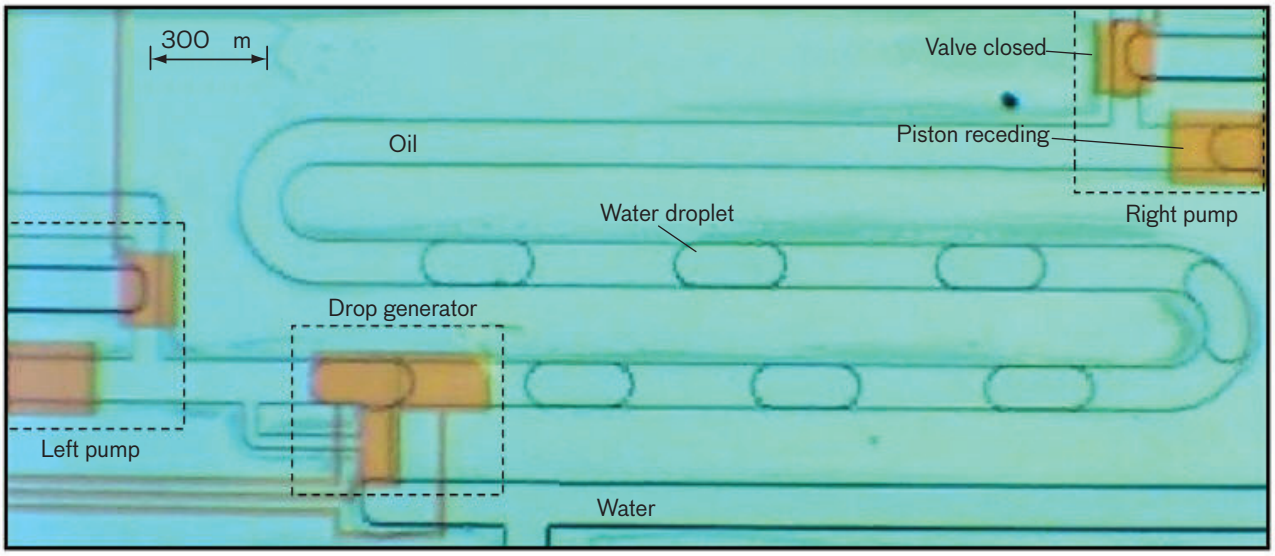

FIGURE 7. The integrated microfluidic system shown in this top-down photo consists of a drop generator and two piston/valve pumps. Eight water drops are created and move left to right with the right-side pump working in "pull" mode.

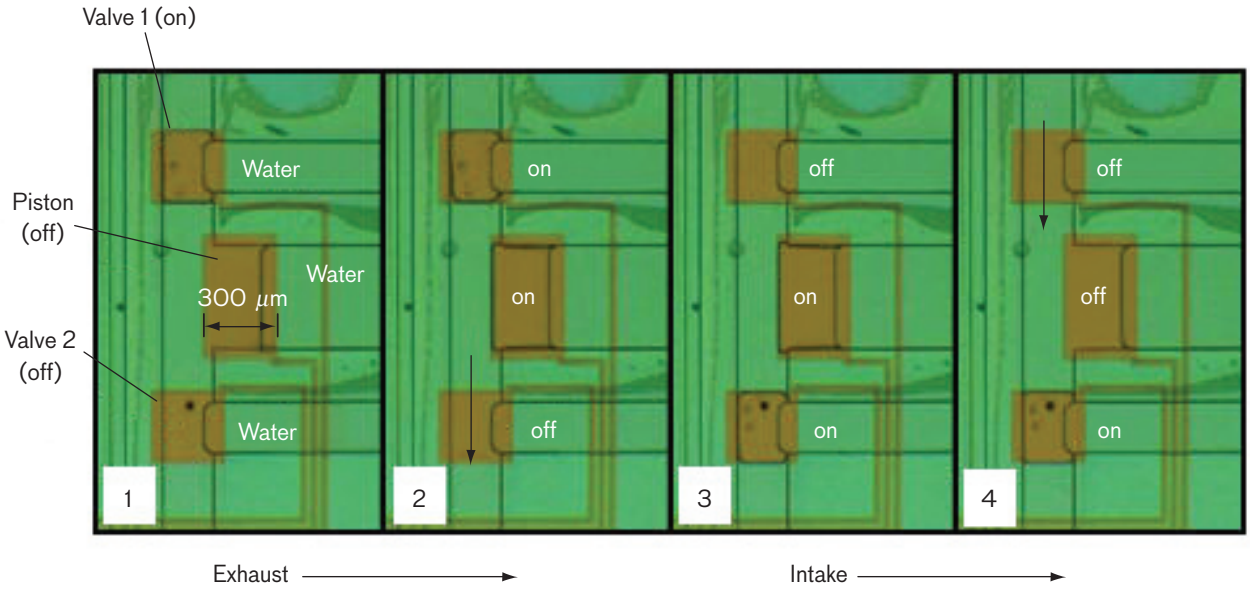

FIGURE 8. This top-down photo of a displacement oil pump shows the exhaust and intake pumping cycle. The design consists of two valve electrodes and a piston electrode: (1) valve 1 on, water blocking oil channel; (2) valve 1 on, piston actuated, displacing oil downstream; (3) valve 1 off, opening upstream oil channel; valve 2 on, blocking downstream channel; (4) piston off, interface retreats (3 to 4), drawing oil into the pump chamber.

capability. In this design, the oil phase is the working fluid and is pumped continuously through the proper placement of electrodes and sequencing of the electrode timing. The design consists of two valves and a piston.

Figure 8 shows the implementation of an oil pump going through the exhaust and intake cycle. Properly timing the sequence of the valves and piston actuations allows the continuous pumping of oil. One experiment for this pump geometry—in which we set V = 85 V dc, P_b = 6.5 kPa, and piston on/off timing at 0.15 s—resulted in a maximum flow rate of 10 nL/s and an estimated power of 10 μW.

Design 3: Water Pump. The water pump functions similarly to the oil pump. However, there are important differences in engineering the channel heights. In this design, the pump chamber is at a different channel height from that of the valves and piston. To make fabrication easier, we kept the chamber height at the same height as the water channels (22 μm). This design allows a finite volume of water to remain locked in the pump chamber without bleeding out into the valve region.

Figure 9 shows the water pump going through the intake and exhaust cycle. When a potential is applied to the valve electrode, water fills the valve region and the water valve is open. When the potential is removed, the water retreats from the valve region so that the flow of water is blocked by oil. The piston draws water into the pump chamber during actuation and dispenses water when the potential is removed. Properly timing the sequence of the valves and piston actuations can pump water continuously. For the pump geometry shown in Figure 9—operating at V = 85 V dc, P_b = 8.0 kPa, and piston on/off timing = 2 s—we achieved a flow rate of about 1 nL/s and a power output of about 2 μW.

Next Steps: Applications

The transport concepts and micropumps developed in this effort demonstrated the proof of concept of using the deformation of a liquid interface to pump fluid. Our technology has the advantage of being compact relative to the amount of work it can produce. In addition, it is easily scalable both in size and power needed. We made no effort in this work to reduce the operating voltage. In earlier studies, we routinely demonstrated electrowetting actuation below 20 V [29, 30], opening up the possibility of using battery power. Looking forward, we expect to further reduce both the package size and operating voltage, moving this technology well ahead of many current micropump designs.

We believe that these transport concepts will enable many microfluidic applications and will form a basis for

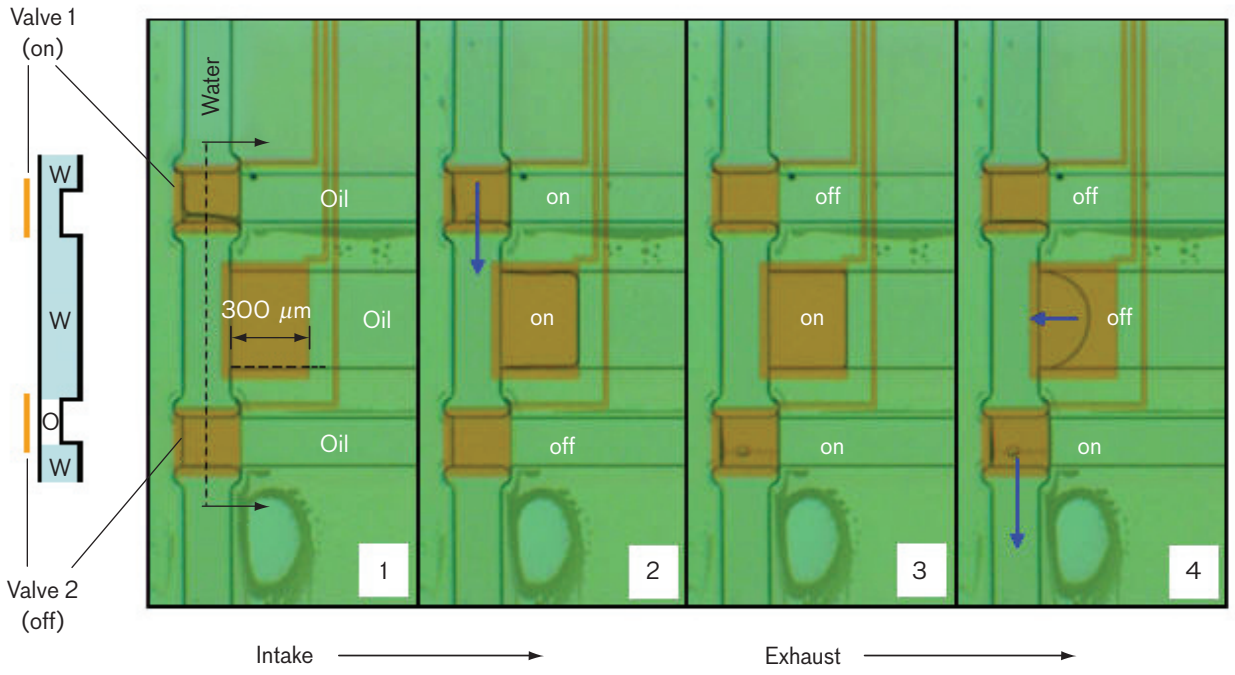

FIGURE 9. The displacement water pump consists of two valve electrodes and a piston electrode. The pump chamber region has a different channel height from that of the valve region. The intake and exhaust pumping cycle: (1) water valve open, valve 1 on; (2) piston actuated, drawing water into pump chamber; (3) valve 1 off, valve 2 on; (4) piston off, interface retreats, forcing water down the channel.

a multitude of biological sensing devices and systems. Future work will focus on integrating these pumping and transport concepts into such systems. Designs for external blood sensors using electrowetting are being developed. The roadmap envisioned is to develop external sensors for monitoring biofluids, then to extend their use to implantable biofluid sensors, and finally to develop implantable drug delivery systems with biosensors to assess when and how much to dispense.

Applications envisioned are not limited to medical diagnostics tools. Other areas being explored include developing pathogen detection sensors, which could serve the mission of chemical and biological defense. One logical technology to partner with is the bioelectronic sensor CANARY [35], which provides speed and sensitivity for identifying pathogens and toxins. Using our microfluid transport methods can help develop a true lab-on-a-chip platform. This platform will allow the development of extremely small, portable sensor systems.

Besides the engineering problems of the integration of various systems needed to develop these sensors, there are still several technical challenges associated with electrowetting. Environmental concerns, in particular temperature effects on electrowetting behavior, need to be understood. The surface tension of a liquid is a strong function of temperature, and since this is a surface-tension-dominated effect, how this process is affected by temperature changes needs to be understood, especially for a portable or implantable device. The other technology challenge is the limited material choices. Currently, only a few fluoropolymers work well with the electrowetting process, from both the convenience of fabrication and the delivery of the desired electrowetting performance, i.e., reversibility.

For electrowetting to be a viable technology over a broader range of applications, research in improving the electrical properties (higher dielectric constant), mechanical properties (functional over a greater temperature range), and biocompatibility is required. Materials research is currently under way at several universities [36]. Despite these technical challenges, electrowetting offers arguably the most versatile technique that can be used to manipulate fluids on a microscale.

Acknowledgments

The authors thank Behrouz Abedian of Tufts University for his many technical contributions on this project. We also thank the staff of the Microelectronics Laboratory and the staff from other clean rooms used during this effort who assisted in fabrication and test setup. ■

REFERENCES

1. G. Whitesides, "The Origins and the Future of Microfluidics," *Nature,* vol. 442, 2006, pp. 368–373.
2. D.J. Laser and J.G. Santiago, "A Review of Micropumps," *J. Micromech. Microeng.,* vol. 14, no. 6, 2004, pp. R35–R64.
3. C.R. Buie, D. Kim, S. Litster, and J.G. Santiago, "An Electro-Osmotic Fuel Pump for Direct Methanol Fuel Cells," *Electrochem. Solid-State Lett.,* vol. 10, no. 11, 2007, pp. B196–B200.
4. J. Wu, "AC Electro-Osmotic Micropump by Asymmetric Electrode Polarization," *J. Applied Physics,* vol. 103, no. 2, 2008, 024907.
5. W.-H. Huang, F. Ai, Z.-L. Wang, and J.-K. Cheng, "Recent Advances in Single-Cell Analysis Using Capillary Electrophoresis and Microfluidic Devices," *J. Chromatography B,* vol. 866, no. 1–2, 2008, pp. 104–122.
6. N. Pamme, "Magnetism and Microfluidics," *Lab Chip,* vol. 6, 2006, pp. 24–38.
7. M.F. Schneider, Z. Guttenberg, S.W. Schneider, K. Sritharan, V.M. Myles, U. Pamukci, and A. Wixforth, "An Acoustically Driven Microliter Flow Chamber on a Chip (μFCC) for Cell-Cell and Cell-Surface Interaction Studies," *ChemPhysChem,* vol. 9, no. 4, 2008, pp. 641–645.
8. Z. Jiao, N.-T. Nguyen, and X. Huang, "Thermocapillary Actuation of Liquid Plugs Using a Heater Array," *Sens. Actuators A,* vol. 140, no. 2, 2007, pp. 145–155.
9. N.-T. Nguyen, X. Huang, and T. K. Chuan, "MEMS-Micropump: A Review," *J. Fluids Engineering,* vol. 124, no. 2, 2002, pp. 384–392.
10. H. van Lintel, F. van de Pol, and S. Bouwstra, "A Piezoelectric Micropump Based on Micromachining of Silicon," *Sens. Actuators A,* vol. 15, 1988, pp. 153–167.
11. F. Mugele and C.J. Baret, "Electrowetting from Basics to Applications," *J. Phys. Condens. Matter,* vol. 17, 2005, pp. R705–R774.
12. H. Moon, S.K. Cho, R.L. Garrell, and C.-J. Kim, "Low Voltage Electrowetting-on-Dielectric," *J. Appl. Phys.,* vol. 92, no. 7, 2002, pp. 4080–4087.
13. T. Jones, "An Electromechanical Interpretation of Electrowetting," *J. Micromech. Microeng.,* vol. 15, 2005, pp. 1184–1187.
14. S. Kuiper and B.H.W. Hendriks, "Variable-Focus Liquid Lens for Miniature Cameras," *Appl. Phys. Lett.,* vol. 85, no. 7, 2004, pp. 1128–1130.
15. B. Berge and J. Peseux, "Variable Focal Lens Controlled by an External Voltage: An Application of Electrowetting," *Eur. Phys. J. E,* vol. 3, 2000, pp. 159–163.
16. Y.H. Chang, K. Mohseni, and V. Bright, "Fabrication of Tapered SU-8 Structure and Effect of Sidewall Angle for Variable Focus Microlens Using EWOD," *Sens. Actuators A,* vol. 136, 2007, pp. 546–553.
17. R. Shami, D. Andelman, B. Berge, and R. Hayes, "Water, Electricity, and Between. On Electrowetting and its Applications," *Soft Matter,* vol. 4, no. 1, 2008, pp. 38–45.
18. R. van Dijk, B.J. Feenstra, R.A. Hayes, I.G.J. Camps, R.G.H. Boom, M.M.H. Wagemans, A. Giraldo, B.V.D. Heijden, R. Los, and H. Feil, "Gray Scales for Video Applications on Electrowetting Displays," *SID Symp. Digest of Technical Papers,* vol. 37, no. 4, 2006, pp. 1926–1929.
19. B. Sun, K. Zhou, Y. Lao, J. Heikenfeld, and W. Cheng, "Scalable Fabrication of Electrowetting Displays with Self-Assembled Oil Dosing," *Appl. Phys. Lett.,* vol. 91, no. 1, 2007, 011106/1–3.
20. K. Blankenbach, A. Schmoll, A. Bitman, F. Bartels, and D. Jerosch, "Novel Electrowetting Displays," *SID Symp. Digest of Technical Papers,* vol. 38, no. 1, 2007, pp. 618–621.
21. H. Hosono, W. Satoh, J. Fukuda, and H. Suzuki, "On-Chip Handling of Solutions and Electrochemiluminescence Detection of Amino Acids," *Sens. Actuators B,* vol. 122, no. 2, 2007, pp. 542–548.
22. V. Srinivasan, V. Pamula, M. Pollack, and R. Fair, "A Digital Microfluidic Biosensor for Multianalyte Detection," *Proc. IEEE 16th Annual Int. Conf. on Micro Electro Mechanical Systems,* Kyoto, Jan. 19–23, 2003, pp. 327–330.
23. S.K. Cho, H. Moon, and C.-J. Kim, "Creating, Transporting, Cutting, and Merging Liquid Droplets by Electrowetting-Based Actuation for Digital Microfluidic Circuits," *J. Microelectromech. Syst.,* vol. 12, no. 1, 2003, pp. 70–80.
24. M.G. Pollack, A.D. Shenderov, and R.B. Fair, "Electrowetting-Based Actuation of Droplets for Integrated Microfluidics," *Lab Chip,* vol. 2, 2002, pp. 96–101.
25. C.G. Cooney, C.Y. Chen, M.R. Emerling, A. Nadim, and J.D. Sterling, "Electrowetting Droplet Microfluidics on a Single Planar Surface," *Microfluid Nanofluid,* vol. 2, 2006, pp. 435–446.
26. Y.-H. Chang, G.-B. Lee, F.-C. Huang, Y.-Y. Chen, and J.-L. Lin, "Integrated Polymerase Chain Reaction Chips Utilizing Digital Microfluidics," *Biomed. Microdevices,* vol. 8, 2006, pp. 215–225.
27. D. Jary, A. Chollat-Namy, Y. Fouillet, J. Boutet, C. Chabrol, G. Castellan, D. Gasparutto, and C. Pepponet, "DNA Repair Enzyme Analysis on EWOD Fluidic Microprocessor," *NSTI Nanotech 2006 Tech. Proc.,* vol. 2, 2006, pp. 554–557.
28. U.-C. Yi and C.-J. Kim, "Soft Printing of Droplets Pre-Metered by Electrowetting," *Sens. Actuators A,* vol. 114, nos. 2–3, 2004, pp. 347–354.
29. J. Kedzierski and S. Berry, "Engineering the Electrocapillary Behavior of Electrolyte Droplets on Thin Fluoropolymer Films," *Langmuir,* vol. 22, 2006, pp. 5690–5696.
30. S. Berry, J. Kedzierski, and B. Abedian, "Low Voltage Electrowetting Using Thin Fluoropolymer Films," *J. Colloid Interface Sci.,* vol. 303, 2006, pp. 517–524.

31. S. Berry, J. Kedzierski, and B. Abedian, "Irreversible Electrowetting on Thin Fluoropolymer Films," *Langmuir,* vol. 23, 2007, pp. 12429–12435.
32. Y. Zhao and S.K. Cho, "Micro Air Bubble Manipulation by Electrowetting on Dielectric (EWOD): Transporting, Splitting, Merging and Eliminating of Bubbles," *Lab Chip,* vol. 7, 2007, pp. 273–280.
33. A.W. Adamson and A. Gast, *Physical Chemistry of Surfaces,* 6th ed. (Wiley, New York, 1997).
34. S. Berry, "Electrowetting Phenomenon for Microsized Fluidic devices," Ph.D. thesis, Tufts University, 2008.
35. M.S. Petrovick, J.D. Harper, F.E. Nargi, E.D. Schwoebel, M.C. Hennessy, T.H. Rider, and M.A. Hollis, "Rapid Sensors for Biological-Agent Identification," *Linc. Lab. J.,* vol. 17, no. 1, 2007, pp. 63–84.
36. M.K. Kilaru, G. Lin, J.E. Mark, and J. Heikenfeld, "Strong Charge Trapping and Bistable Electrowetting on Nanocomposite Fluoropolymer: $BaTiO_3$ Dielectrics," *Appl. Phys. Lett.* vol. 90, 2007, 212906.

ABOUT THE AUTHORS

Shaun Berry is a staff member in the Advanced Silicon Technology Group, where he is involved with the design, fabrication, and characterization of microfluidic and microelectromechanical systems (MEMS). He has a doctorate in mechanical engineering from Tufts University.

Jakub Kedzierski is an assistant group leader for the Advanced Silicon Technology Group. He has a doctorate in electrical engineering from the University of California, Berkeley.